

Characterization of a TET-like Aminopeptidase Complex from the Hyperthermophilic Archaeon *Pyrococcus horikoshii*[†]

M. Asunción Durá,[‡] Veronique Receveur-Brechot,[§] Jean-Pierre Andrieu,[‡] Christine Ebel,[‡] Guy Schoehn,[‡] Alain Roussel,[§] and Bruno Franzetti^{*‡}

Institut de Biologie Structurale, J.-P. Ebel CEA-CNRS-UJF, Grenoble, France, and Architecture et Fonction des Macromolécules Biologiques, UMR-6098, CNRS, Marseille, France

Received October 22, 2004; Revised Manuscript Received December 17, 2004

ABSTRACT: *Pyrococcus horikoshii* open reading frame PH1527 encodes a 39014 Da protein that shares about 30% identity with endoglucanases and members of the M42 peptidase family. Analytical ultracentrifugation and electron microscopy studies showed that the purified recombinant protein forms stable, large dodecameric complexes with a tetrahedral shape similar to the one described for DAP, a deblocking aminopeptidase that was characterized in the same organism. The two related proteins were named PhTET1 (for DAP) and PhTET2 (for PH1527). The substrate specificity and the mode of action of the PhTET2 complex were studied in detail and compared to those of PhTET1 and other assigned M42 peptidases. When assayed with short chromogenic peptides, PhTET2 was found to be an aminopeptidase, with a clear preference for leucine as the N-terminal amino acid. However, the enzyme can cleave moderately long polypeptide substrates of various compositions in a fairly unspecific manner. The hydrolytic mechanism was found to be nonprocessive. The enzyme has neither carboxypeptidase nor endoproteolytic activities, and it is devoid of N-terminal deblocking activity. PhTET2 was inhibited in the presence of EDTA and bestatin, and cobalt was found to be an activating metal. The PhTET2 protein is a highly thermostable enzyme that displays optimal activity around 100 °C over a broad pH array.

Proteases are found in every cell and are critical to the maintenance of cellular function. They break down unneeded or abnormal polypeptides or peptide-based nutrients within or outside the cell. Proteases range from simple monomeric hydrolases to complex, multisubunit structures with molecular masses in the order of 1 MDa (1). Some of these high molecular weight proteases are self-compartmentalized and accomplish key cellular functions in the control of the half-life of proteins in the cytosol (2). Broadly, cytosolic protein degradation can be divided into four steps. (i) Proteins targeted for degradation are initially unfolded by ATP-dependent proteases belonging to the Lon/Clp family in bacteria or 26S proteasomes in eukaryotes (3). (ii) These enzymes also make the initial endoproteolytic attack in the polypeptide. The average length of peptides released by these enzymes ranges from 3 to 25 amino acids (4, 5). (iii) These longer peptides are trimmed into smaller peptides (less than 10 amino acids) by the action of endopeptidases (6–8) and tripeptidyl- and dipeptidylpeptidases (9–12). (iv) Finally, aminopeptidases, carboxypeptidases, and di- and tripeptidases digest these peptides into amino acids (7, 13). Most of the amino acid recycling enzymes acting in the last steps of the

cytosolic protein degradation pathway are metallopeptidases (7, 9, 14–16).

In the course of the purification of the proteasome from the extreme halophilic archaeon *Haloarcula marismortui*, we detected TET, a new type of giant protease that forms a tetrahedral structure and can cleave large substrates such as the 6–12 amino acid long proteasome reaction products (13). The protein sequence of *H. marismortui* TET (HmTET)¹ is homologous to the protein product of the *Halobacterium* sp. *celM* gene that was originally designated as a putative endoglucanase (17). However, the *Halobacterium* protein appears in the MEROPS classification of peptidases² (18) as a TET aminopeptidase belonging to the M42 family in the MH clan of metallopeptidases. The exact role of such intracellular ATP-independent proteases forming large oligomeric edifices is still not well defined. To elucidate the

[†] The authors thank the CNRS and the Rhône-Alpes Region for financial support.

* Address correspondence to this author at the Institut de Biologie Structurale, J.-P. Ebel CEA-CNRS-UJF, UMR-5075, 41 rue Jules Horowitz, 38027 Grenoble Cedex 1, France. Telephone: +33 438 789 570. Fax: +33 438 785 494. E-mail: franzetti@ibs.fr.

[‡] Institut de Biologie Structurale.

[§] Architecture et Fonction des Macromolécules Biologiques.

¹ Abbreviations: HmTET, *Haloarcula marismortui* TET; HTET, *Halobacterium* sp. TET; DAP, deblocking aminopeptidase; PhTET1, *Pyrococcus horikoshii* TET1 (deblocking aminopeptidase); PhTET2, *P. horikoshii* TET2; GluAP, *Lactococcus lactis* glutamyl aminopeptidase; API, *Bacillus stearothermophilus* aminopeptidase I; bLAP, bovine lens leucyl aminopeptidase; AAP, *Aeromonas* aminopeptidase; SGAP, *Streptomyces griseus* aminopeptidase; pNA, 4-nitroaniline; AMC, 7-amino-4-methylcoumarin; βNA, 2-naphthylamine; Ac, acetyl; Z, benzyloxycarbonyl; Suc, 3-carboxypropionyl; PIPES, piperazine-1,4-bis(2-ethanesulfonic acid); HEPES, 4-(2-hydroxyethyl)piperazine-1-ethanesulfonic acid; TAPS, N-[tris(hydroxymethyl)methyl]-3-aminopropanesulfonic acid; FITC, fluorescein isothiocyanate; EDTA, ethylenediaminetetraacetate.

² This report follows the MEROPS classification of peptidases (available on the World Wide Web at merops.sanger.ac.uk). This system groups peptidases with significant sequence similarity into a family and assigns families of common evolutionary origin to a clan.

common function of these complexes in the cell, it is important to characterize TET protease homologues from other organisms and to identify the substrates that they can manipulate.

In the genome of the hyperthermophilic archaeon *Pyrococcus horikoshii* two open reading frames were detected coding for proteins that have 47% (PH1527) and 43% (PH0519) homology to *Halobacterium* TET aminopeptidase (HTET). PH0519 encodes a thermostable aminopeptidase described first by Ando et al. (19) and called PhDAP by Onoe et al. (20) due to its acylamino acid releasing activity similar to that found by Tsunasawa (21) in the deblocking aminopeptidase (DAP) from *Pyrococcus furiosus*. We recently solved the X-ray crystal structure of PhDAP.³ It shows that this protein forms dodecameric tetrahedral complexes analogous to the ones discovered while studying HmTET (13). Here we show that the PH1527 product shares with HmTET and PhDAP their characteristic tetrahedral shape in solution, in agreement with the recently published X-ray structure of the PH1527 protein (22). Consequently, hereafter we will designate PhDAP as PhTET1 and the PH1527 product as PhTET2. The specificity, the mode of action, and the enzymatic activity of this second TET complex from *P. horikoshii* are presented and discussed in this paper.

EXPERIMENTAL PROCEDURES

Protein Expression and Purification. We used the *Escherichia coli* strain BL21 pLys S (DE3) (Novagen) for expression of recombinant PhTET2. The cells were grown in 1 L of 2YT medium (1% yeast extract, 1.6% tryptone, and 0.5% NaCl) containing ampicillin (100 μ g/mL) and chloramphenicol (34 μ g/mL). After incubation with shaking at 37 °C until the A_{600} reached 0.6–1.0, the induction was carried out by adding isopropyl β -D-thiogalactopyranoside at a final concentration of 0.05 mM and shaking for 4 h at 37 °C. The induced cells were harvested by centrifugation. The pellets were then maintained at –80 °C overnight. The complete disruption of the cells was achieved by a French press after thawing and suspension in 50 mL of 50 mM Tris-HCl and 150 mM NaCl, pH 8.0, supplemented with DNase I and RNase. The crude extract was heated at 85 °C for 30 min. The lysate was clarified by centrifugation at 25000g for 30 min. The supernatant was loaded on a HiTrap Q column (Amersham Pharmacia Biotech). The column was eluted with a linear gradient (0–1.5 M NaCl in 50 mM Tris-HCl, pH 8.0). The fractions containing protein of similar mass (37–39 kDa) according to SDS–PAGE were combined and concentrated using an Amicon cell (Millipore) with a molecular mass cutoff of 30 kDa. The protein was then loaded onto a Superdex 200 Hiload 26/60 column (Amersham Pharmacia Biotech). An elution peak corresponding to a molecular mass around 400 kDa was observed. According to SDS–PAGE and to N-terminal sequencing, the corresponding fractions contained pure PhTET2. The fractions were pooled and kept at 5 °C after concentration to about 10 mg/mL. The protein concentration was measured using the Bio-Rad protein assay reagent (Bio-Rad).

Analytical Ultracentrifugation. Sedimentation velocity experiments were performed using a Beckman XL-I analyti-

cal ultracentrifuge and an AN-60 TI rotor (Beckman Instruments). The experiments were carried out at 20 °C in 50 mM Tris-HCl and 150 mM NaCl, pH 7.5. The sample of 400 μ L at a protein concentration of 0.2 mg/mL was loaded into 1.2 cm path length cells and centrifuged at 42000 rpm. Scans were recorded at 275 nm every 5 min using a 0.003 cm radial spacing. The sedimentation profiles were analyzed in terms of size distribution analysis using Sedfit⁴ (23). We estimated the partial specific volume of the protein to be 0.7485 mL/g and the solvent density and viscosity to be 1.006 g/mL and 1.03 mPa·s, respectively, using the Sednterp software from Hayes, Laue, and Philo.⁵ We used 200 generated sets of data on a grid of 300 radial points, calculated using a frictional ratio of 1.25 for sedimentation coefficients at 20° comprised between 2 and 30 S and, for the regularization procedure, a confidence level of 0.7.

Electron Microscopy. Protein samples at approximately 0.1 mg/mL in 50 mM Tris-HCl and 150 mM NaCl, pH 7.5, were applied to the clean side of carbon on mica (carbon/mica interface) and negatively stained with 2% uranyl acetate. Micrographs were taken under low-dose conditions with a JEOL 1200 EX II microscope at 100 kV and a nominal magnification of 40000 times on SO163 Kodak film.

Determination of PhTET2 Activity on Synthetic Chromogenic and Fluorogenic Compounds. PhTET2 hydrolytic activity on synthetic chromogenic and fluorogenic compounds was determined using different aminoacyl-pNAs, aminoacyl-AMCs, and peptides (listed in Table 1) through the following standard assay procedure. Reactions were initiated by addition of the enzyme (0.2 or 1 μ g/mL) to a prewarmed mixture containing the chromogenic or fluorogenic compound in 50 mM PIPES, 150 mM KCl, and 1 mM CoSO₄, pH 7.5, and covered by a layer of mineral oil to avoid water evaporation. Incubations were performed at 90 °C for 0.5, 5, or 10 min, and reactions were stopped by cooling at 0 °C. The quantity of pNA, AMC, or β NA liberated was measured in a VICTOR 1420 multilabel counter (Wallac). For pNA, absorbance was determined at 405 nm, and for AMC and β NA, fluorescence was measured using excitation and emission wavelengths of 355 and 460 nm, respectively. Due to the higher signal response of the AMC derivatives with respect to the pNA ones, the former were used at lower concentrations, and incubation times were accordingly reduced. Four replicates and four controls were assayed for each experimental point.

For the study of Ala-Ala-Phe-AMC degradation by PhTET2, the enzyme (2 μ g/mL) was incubated with the substrate (0.5 mM) using the standard assay conditions. At determined times, 80 μ L aliquots were removed from the reaction mixture and added to 200 μ L of cold acetonitrile in order to stop the reaction and precipitate the protein (24). Samples were maintained at 4 °C for 15 min, and protein was removed by centrifugation. Two hundred fifty microliters of supernatant was dried under vacuum. Solids were then dissolved in the same volume of Beckman analysis buffer, and the amino acids and small peptides present in each sample were quantified on a Model 7300 Beckman amino

⁴ Available on the World Wide Web at www.analyticalultracentrifugation.com.

⁵ Available on the World Wide Web at www.bbri.org/RASMB/rasmb.html.

³ F. M. D. Vellieux, V. Receveur-Brechot, G. Schoehn, M. A. Durá, A. Roussel, and B. Franzetti, unpublished results.

acid analyzer, using the standard sodium citrate elution buffer system. Calibrations were made using aliquots of four standard solutions. The quantity of AMC cleaved by the enzyme was measured directly in aliquots of the reaction mixture as described previously. Each sample was accompanied by an appropriate control.

Study of PhTET2 Activity on Peptides. To assay the proteolytic activity of PhTET2 against the peptides listed in Table 2, the enzyme (1 $\mu\text{g/mL}$) was incubated with 0.1 mM peptide in the standard assay conditions. Reaction mixtures contained also 10 μM Trp as internal standard. At determined times, 80 μL aliquots were removed and added to 200 μL of cold acetonitrile. Protein was removed by centrifugation. Two hundred fifty microliters of supernatant was dried under vacuum, and the remaining solids were dissolved in 70 μL of the chromatography initial eluent. Fifty microliters was injected on a $\mu\text{RPC C2/C18 ST}$ column (4.6×100 mm) (Amersham) in an AKTA purifier system (Amersham). Chromatographic conditions were dependent on the peptide mixture, but in all cases eluent A was composed of 0.065% trifluoroacetic acid and 2% acetonitrile in water, and eluent B contained 0.05% trifluoroacetic acid in 80% acetonitrile. Flow was adjusted at 0.5 mL/min, and chromatographic runs were carried out at room temperature. The separated fragments were collected and submitted to N-terminal sequence analysis. This analysis was performed by Edman degradation using an Applied Biosystems gas-phase sequencer, model 492. Phenylthiohydantoin amino acid derivatives were identified and quantified on-line using a model 140C HPLC system (Applied Biosystems) and a model 785A absorbance detector, as recommended by the manufacturer. The generation of free amino acids from Tub-Cter was determined as described previously. Each sample was accompanied by an appropriate control.

Effect of Metal Cations on PhTET2 Activity. The metal cations (listed in Table 3) were incubated at 0.5 mM concentration with the enzyme (1 $\mu\text{g/mL}$) and the substrate (5 mM Leu-pNA) in 50 mM HEPES and 150 mM KCl, pH 7.5, at 80 °C for 10 min. The reactions were stopped by cooling at 0 °C, and pNA absorbance was measured as previously described. Four replicates and four controls were assayed for each experimental point.

Effect of Temperature and pH on PhTET2 Activity. The effect of pH on PhTET2 activity was determined in the pH range from 6.0 to 9.0. The buffers used were 50 mM PIPES, pH 6.0–7.5, 50 mM HEPES, pH 7.0–8.0, and 50 mM TAPS, pH 8.0–9.0. The effect of temperature on the activity was measured in the range from 60 to 99.9 °C. In all cases, the enzyme (0.5 $\mu\text{g/mL}$) was incubated with 5 mM substrate (Leu-pNA). To assess the effect of pH on activity, incubations were done at 80 °C for 5 min in the indicated buffers to which 150 mM KCl and 5 mM CoSO_4 were added. When the effect of temperature was determined, incubations were performed in 50 mM PIPES, 150 mM KCl, and 5 mM CoSO_4 , pH 7.5. The reactions were stopped by cooling at 0 °C, and pNA absorbance was measured. Four replicates and four controls were assayed for each experimental point.

PhTET2 Thermal Stability. The effect of temperature on PhTET2 stability was assayed by incubating the enzyme (4 $\mu\text{g/mL}$) at several temperatures (listed in Table 4) in 50 mM PIPES, 150 mM KCl, and 1 mM CoSO_4 , pH 7.5. Five-microliter aliquots were taken at different time intervals, and

the remaining aminopeptidase activity was assayed against 5 mM Leu-pNA by incubation at 90 °C for 5 min in 95 μL of the same buffer. Reactions were stopped by cooling at 0 °C, and pNA absorbance was measured. Four replicates (samples plus controls) were assayed for each experimental point. The remaining activity at each time interval was expressed as a percentage of the activity present at zero time (100%). Half-lives were calculated from a first-order exponential decay fit to the six experimental points obtained for each temperature.

Effect of Chemical Agents on PhTET2 Activity. The enzyme (0.2 $\mu\text{g/mL}$) was incubated together with the chemical agents listed in Table 5 and 5 mM Leu-pNA following the standard assay procedure. pNA absorbance was measured as described. Four replicates and four controls were assayed for each experimental point.

RESULTS

The Protein Encoded by PH1527 Belongs to the M42 Peptidase Family. A BLAST search for protein homologous to HTET showed 32% identity (47% homology) with the gene product of the *P. horikoshii* PH1527 open reading frame, defined by the EMBL/GenBank as a 353 amino acid long hypothetical Frv operon protein FrvX of 39014 Da. Following the MEROPS classification of peptidases in evolutionary clans and according to its family assignment criteria based on sequence similarities (18), the PH1527 gene product belongs to family M42 in the clan MH of metallopeptidases. The sequence alignments against three other assigned proteins of the M42 family are shown in Figure 1. Metallopeptidases are among the hydrolases in which the nucleophilic attack on a peptide bond is mediated by a water molecule. A divalent metal cation, usually zinc but sometimes cobalt, manganese, nickel, or copper, activates the water molecule (25). Peptidases from clan MH have cocatalytic metal ions; that is to say, they require two metal ions acting together for full activity (26). The recently solved X-ray crystal structures of PhTET1³ and FrvX (22) confirm that, in the case of the proteins from family M42, the metal binding residues are two histidines, two aspartates, and one glutamate (Figure 1). The active site also contains one aspartyl and one glutamyl residue involved in catalysis.

The Protein Encoded by PH1527 Is a Tetrahedral Dodecameric Complex. The recombinant PH1527 protein was purified from *E. coli* extracts by heat shock denaturation of the bulk *E. coli* proteins followed by ion-exchange and gel filtration chromatographies. The protein eluted as a well-separated high molecular mass complex from the gel filtration column, suggesting that it was a homooligomeric assembly (data not shown). We examined the size of the purified complex by sedimentation velocity experiments. Figure 2A shows the protein encoded by PH1527 as quite homogeneous in solution. A main peak at 15.2 S is revealed in the analysis in terms of a distribution of sedimentation coefficients, corresponding to more than 85% of the absorbance. The value of 15.2 S corresponds, in the hypothesis of a noninteracting globular compact particle, to a molar mass of 475 kDa (12.2 subunits).

In electron micrographs, the quaternary structure of the purified protein appeared essentially in negative stain as a hollow-shaped complex of homogeneous size (Figure 2B). The dimensions and the shape of the edifice are identical to

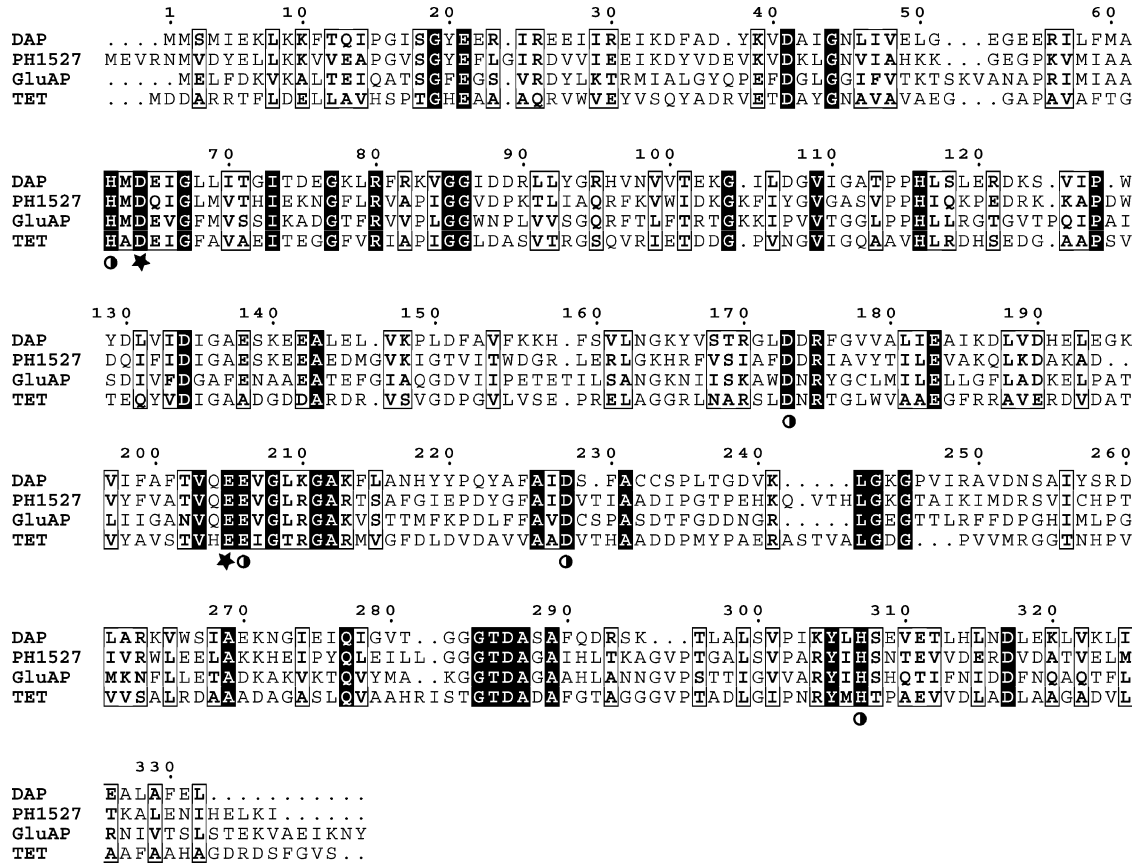


FIGURE 1: The protein encoded by PH1527 is a M42 peptidase homologue. Multiple sequence alignment of three assigned M42 peptidases and the protein encoded by PH1527 was performed using ClustalW. The conserved metal binding residues are indicated by a ball and the catalytic residues by a star [according to the MEROPS database assignment (18)]. The abbreviations and GenBank accession numbers of sequences are as follows: DAP, *P. horikoshii* deblocking aminopeptidase (AP000006); PH1527, *P. horikoshii* uncharacterized TET-like protein (059196); TET, TET aminopeptidase from *Halobacterium* sp. (AE005064); and GluAP, the glutamyl aminopeptidase from *L. lactis* (X81089).

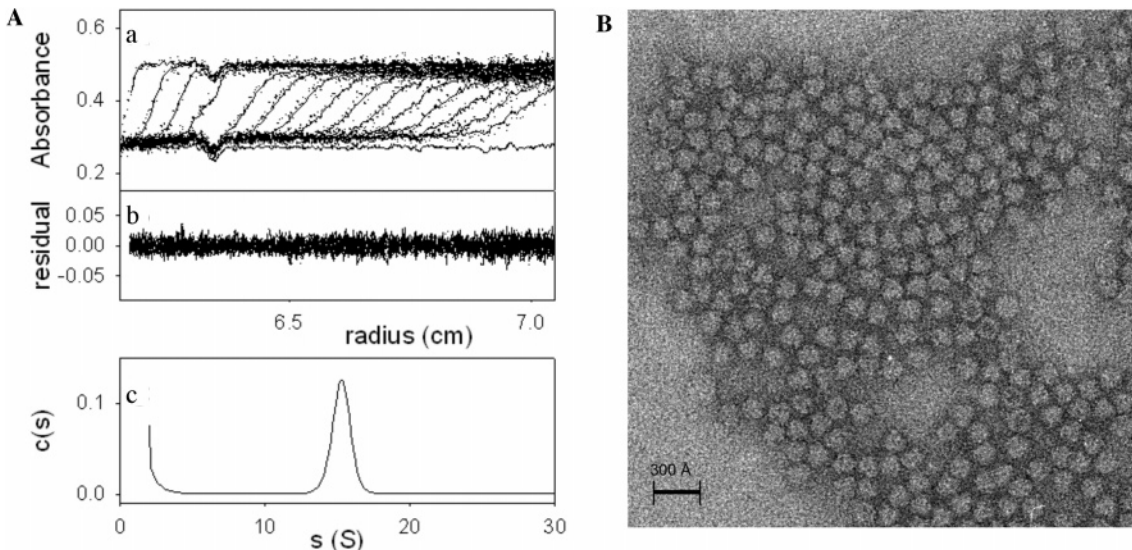


FIGURE 2: Characterization of the PH1527 protein as a TET-like complex. (A) Sedimentation velocity of the purified complex: (a) Superposition of the experimental (dots) and modeled (continuous lines) sedimentation profiles: the last profile corresponds to 73 min of sedimentation at 42000 rpm and 20 °C. The evaluation of the systematic time-independent noise is also shown as a continuous line. (b) Superposition of the difference between the experimental and modeled profiles. (c) Result of the analysis in terms of a distribution of sedimentation coefficients. (B) Electron micrographs of the PH1527 protein edifices. The picture shows a homogeneous population of hollow tetrahedral-shaped complexes.

those of the HmTET (13) and PhTET1³ proteins, which were found to assemble as tetrahedral complexes made of 12 subunits. Therefore, the protein encoded by PH1527 was called PhTET2.

The Purified Dodecameric PhTET2 Complex Is a Leucyl Aminopeptidase. The cleavage specificity of PhTET2 was studied first by using different chromogenic and fluorogenic aminoacyl compounds. As shown in Table 1, the enzyme

Table 1: Activity of PhTET2 on Different Synthetic Chromogenic and Fluorogenic Compounds

substrate	concn (mM)	relative activity ^a (%)
aminoacyl-pNAs		
Leu-pNA	5	100
Met-pNA	5	26.3
Ile-pNA	5	14.3
Ala-pNA	5	10.8
Pro-pNA	5	0.9
Phe-pNA	2	0.8
Gly-pNA	5	0.3
Lys-pNA	5	0.2
Arg-pNA	5	0.1
Asp-pNA	5	0
His-pNA	5	0
Ac-Leu-pNA	2	0
aminoacyl-AMCs		
Ser-AMC	0.5	12.8
Thr-AMC	0.5	6.1
Gln-AMC	0.5	2.8
Val-AMC	0.5	2.1
Tyr-AMC	0.5	0.9
Asn-AMC	0.5	0.3
Orn-AMC	0.5	0.1
Trp-AMC	0.5	0.0
peptides		
Ala-Ala-pNA	5	2.9 ^b
Ala-Ala-Ala-pNA	5	1.3 ^b
Ala-Ala-Phe-AMC	0.5	1.2 ^b
Z-Gly-Gly-Leu-pNA	1	0.2
Suc-Ala-Ala-Phe-pNA	5	0.1
Suc-Ala-Ala-pNA	5	0.0
Z-Leu-Leu-Glu-βNA	1	0.0
Suc-Leu-Leu-Val-Tyr-AMC	0.5	0.0
Suc-Ala-Ala-Phe-AMC	0.5	0.0
Suc-Leu-Tyr-AMC	0.5	0.0
Z-Gly-Gly-Arg-AMC	0.5	0.0
Ala-Pro-pNA	5	0
Z-Ala-Ala-pNA	1	0

^a Expressed as a percentage of the activity against Leu-pNA, which was given a value of 100%. ^b Apparent relative activity (see text).

acted only on a limited number of these aminopeptidase substrates. Optimal amidolytic activity was observed against Leu-pNA. This compound was cleaved almost 4-fold more efficiently than any of the other substrates tested. Met-, Ile-, and Ala-pNA and Ser-AMC were hydrolyzed less efficiently, and very poor or no activity was detected against the other aminoacyl-pNA or aminoacyl-AMC assayed.

PhTET2 Is a Strict Aminopeptidase Devoid of N-Terminal Deblocking Activity. Exopeptidase activity and specificity depends on the sequence composition of the target peptide, and some aminopeptidases have been shown to exhibit also endopeptidase or di/tripeptidyl peptidase activity that can only be detected by studying the peptide degradation process (11, 27–31). Consequently, PhTET2 activity was assayed by using various chromogenic and fluorogenic peptides. No activity was observed against any of the N-terminal blocked derivatives (Table 1). Moreover, activity against FITC-casein could not be detected relative to control experiments in which chymotrypsin was used (data not shown). We also tested Ala-Ala-pNA, Ala-Ala-Ala-pNA, and Ala-Ala-Phe-AMC [a fluorogenic tripeptidylpeptidase substrate (11)], and we observed that PhTET2 generated pNA or AMC from these substrates, although very slowly (Table 1). To determine if the detected activity was the consequence of a di/tripeptidyl action or was the result of sequential aminopeptidase cuts,

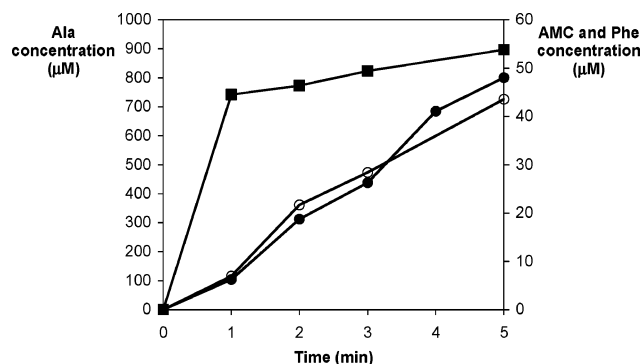


FIGURE 3: Ala-Ala-Phe-AMC degradation by PhTET2. Concentration evolution of the hydrolysis products in the reaction mixture (■, Ala; ●, AMC; ○, Phe).

we investigated the amino acid and small peptide composition of the reaction mixtures at different time points. We could detect neither dipeptides nor tripeptides after analyzing those samples by reversed-phase HPLC (chromogenic substrates/products are not detectable by the method employed). In fact, only amino acids were detected. When Ala-Ala-Phe-AMC was used as a substrate, Ala accumulated very fast in the reaction mixture, and AMC and Phe appeared only after a little lag phase (Figure 3). Moreover, the evolution of these two last products almost coincided, indicating that AMC was liberated at the same time as Phe (i.e., from Phe-AMC). In the same way, we studied the products of the PhTET2-driven hydrolysis of Ala-Ala-pNA. In this case, the quantity of Ala increased linearly with time, accumulating in the reaction mixture 154-fold faster than pNA (not shown), therefore indicating that the enzyme was mostly cleaving the N-terminal Ala directly from the substrate. We analyzed also the possible presence of Ala in the reaction mixture during the incubation of Ala-Pro-pNA with PhTET2; however, we could not detect any degradation product (not shown).

PhTET2 Cleaves Polypeptides by a Nonprocessive Mechanism. For further characterization of the enzyme substrate specificity, we studied the PhTET2-driven degradation of several polypeptides of various lengths listed in Table 2. The goal was to ascertain whether the enzyme was able to degrade long polypeptides and also whether its action followed a processive mechanism; i.e., the enzyme retains partially digested peptide substrates and makes multiple cleavages before the release of products, as, for example, the proteasome and the ClpP protease do (32, 33). PhTET2 action along the 14-residue peptide Tub-Cter is shown in Figure 4. After incubation of PhTET2 with this substrate, the peptides and the amino acids formed were analyzed by reverse-phase HPLC. Several products were obtained, and although the peptide analysis initially showed no presence of the degradation products lacking the two and the three first amino acid residues (Table 2, Figure 4A), the investigation of the amino acids accumulating in the reaction mixture revealed that Asp and Ser were present and that their quantities increased with time (Figure 4B). Therefore, we presume that the Tub-Cter derivatives lacking the two and the three first amino acid residues were not detected during the peptide reverse-phase HPLC due to their fast consumption by the enzyme. This last assumption is supported by the results obtained with the aminoacyl compounds (Table 1) that illustrate a clear PhTET2 preference by hydrophobic or uncharged polar

Table 2: Effect of Peptide Length and Sequence on PhTET2 Activity

peptide name ^a	sequence ^b	significant fragments	% of remaining intact peptide ^c
AIT-Ad2	AITIGNKND (9)	-1, -2, -3	58.8
MBL(176–185)	VDLTGNRLTY (10)	-1	21.4
C12L	CGATPQDLNTML (12)	2 fragments detected	78.1
Tub-Cter	VDSVEGEGEEEEEE (14)	-1, -4, -5, -6	36.9
AntiDAP1	DSEPAAATDVSRFTA (15)	none	100.4
DRO174	GATERFVSPEDVFEVIEEGKSNRHI (27)	1 fragment detected	99.1
RBPCoAtr	MQVTMKSSAVSGQRVGGARVATRSVRRRAQLQV (32)	none	99.2
ColX-NC2	VFYAERYQMPTGIKGPLNTKTQFFIPYTIKSKGI AVR G (39)	none	100.9

^a Peptides were submitted to cleavage by PhTET2, and the reaction products were identified by N-terminal sequencing. ^b The number of amino acid residues is indicated in parentheses. ^c The percentage of remaining intact peptide was determined by comparing its peak area [normalized using the internal standard (Trp) peak area] at 0 and 5 min of incubation.

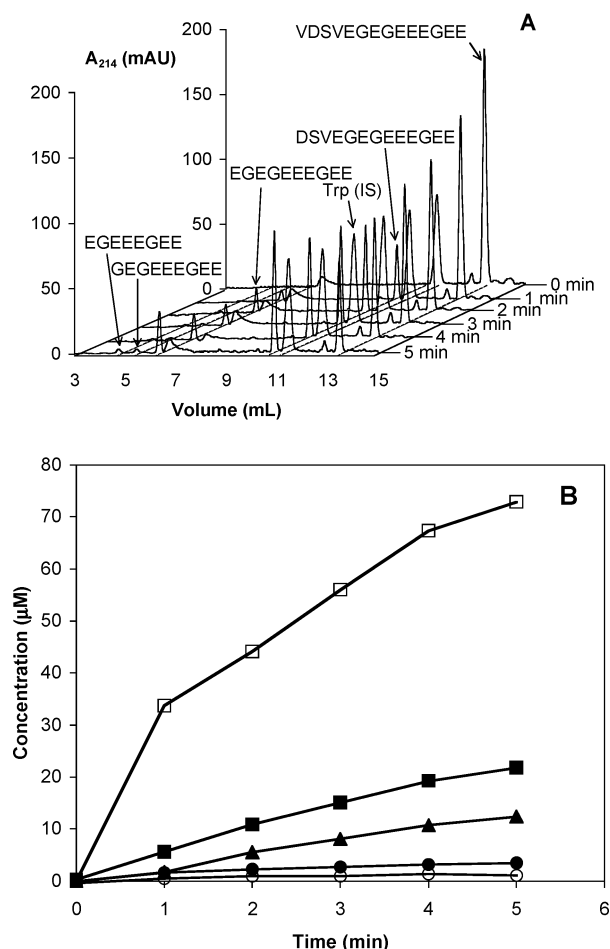


FIGURE 4: PhTET2 acts sequentially on peptide substrates. (A) Chromatographic profiles of the degradation of the 14-residue peptide Tub-Cter. The sequences of the detected accumulating peptides are indicated. Trp was used as internal standard (IS) in order to normalize peak areas. (B) Generation of free amino acids in the reaction mixture due to the action of PhTET2 on Tub-Cter (□, Val; ■, Asp; ▲, Ser; ●, Glu; ○, Gly).

amino acids over charged ones. In the same way, the results shown in Table 2 are consistent with that explanation: (i) We detected several peptide fragments starting by Ile and Thr in the AIT-Ad2 reaction mixture. Given that the initial substrate had an Ala as a first residue, we can envisage that all of these peptides were competing by the enzyme active site (all of them start by an “easy” residue), and that slowed their degradations, so, consequently, they accumulated in the reaction mixture. This interpretation agrees with the relatively low AIT-Ad2 degradation percentage (Table 2). (ii) The only

Table 3: Effect of Metal Cations on PhTET2 Activity

metal	relative activity (%)	metal	relative activity (%)
none	100	Mn ²⁺	49.4
Mg ²⁺	91.7	Zn ²⁺	53.6
Ca ²⁺	97.1	Co ²⁺	539.3

fragment detected during the degradation of the 10-residue peptide MBL starts by an Asp residue, and the peptide AntiDAP1, which also starts by Asp, was not degraded (Table 2). However, this last result can also be related with the apparent inability of PhTET2 for degrading large polypeptides, since the peptides DRO174, RBPCoAtr, and ColX-NC2, which are more than 26 residues long, were not attacked by PhTET2, even though RBPCoAtr and ColX-NC2 start with an easy residue (Met and Val, respectively) (Table 2). On the other hand, the analysis of the quantity of Ser and Asp in the reaction mixture during the degradation of Tub-Cter by PhTET2 indicates a decrease of the Asp/Ser ratio with time (Figure 4B). Since Asp and Ser are the only two amino acids present once per substrate molecule, that observation points toward the absence of PhTET2 processivity on Tub-Cter. The same result is obtained by studying the peak areas of the different peptide products resulting from the degradation of Tub-Cter and also of AIT-Ad2 (not shown). Therefore, the enzyme does not process one substrate molecule completely before starting with another one. Instead, PhTET2 reaction products are generated by multiple rounds of substrate digestion.

PhTET2 Is a Cobalt-Activated Enzyme. The effect of several metal ions on enzyme activity is shown in Table 3. Co²⁺ ion had a clear stimulatory effect on the amidolytic activity. The presence of Zn²⁺ and Mn²⁺ caused around 50% inhibition at 0.5 mM while slight or no effects were observed in the presence of Ca²⁺ and Mg²⁺. Titration of PhTET2 activity against Leu-pNA with Co²⁺ revealed that the cobalt ion optimally enhanced the enzyme activity at 0.5–10 mM concentration (results not shown); hence, concentrations in this range were routinely used in PhTET2 activity assays.

PhTET2 Is a Highly Thermostable Neutral Protease. Using the PhTET2 activity assay with Leu-pNA as a substrate, the enzyme showed optimal amidolytic activity at pH 7.5 in PIPES buffer, and strong activity was still detectable at pH 6 and 9 (Figure 5). Moreover, HEPES buffer was somewhat inhibitory. The temperature dependence of PhTET2 activity at pH 7.5 is also shown in Figure 5. The enzyme was most active around 100 °C. At temperatures lower than 70 °C,

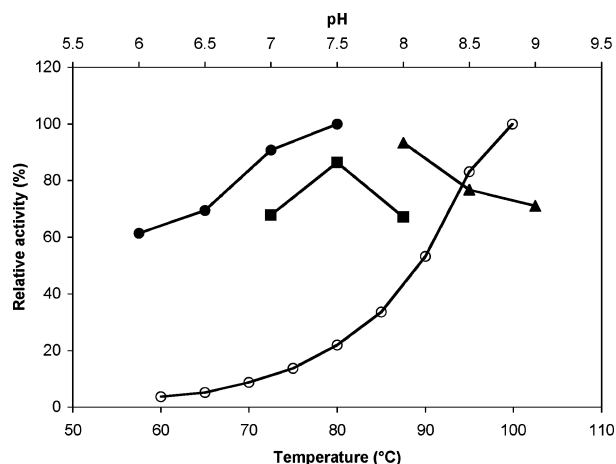


FIGURE 5: Effect of pH and temperature on PhTET2 activity. Evolution of PhTET2 activity as a function of pH in (●) PIPES, (■) HEPES, and (▲) TAPS buffers and as a function of temperature (○).

Table 4: Effect of Different Temperatures on the Half-Life of PhTET2

temp (°C)	half-life	temp (°C)	half-life
100	24.8 min	90	3.00 h
95	59.4 min	80	10.03 h

Table 5: Effect of Different Chemical Agents on PhTET2 Activity

chemical agent	concn (mM)	relative activity (%)	chemical agent	concn (mM)	relative activity (%)
none		100	phosphoramidon	0.5	80.1
antipain	0.1	104.1		1	75.0
bestatin	0.05	35.6		2	71.1
	0.1	22.1	Pefabloc SC	2	93.7
	0.2	15.2	EDTA	1	31.4
chymostatin	0.1	95.0		2	19.5
E-64	0.05	98.3		5	9.6
	0.2	101.9	aprotinin	0.0005	94.4
	1	95.5		0.001	84.7
leupeptin	0.01	95.8		0.01	88.5
	0.05	93.5	puromycin	0.01	96.5
pepstatin	0.001	92.9		0.1	87.1
	0.01	92.4		1	84.9
	0.1	82.6			

less than 10% of the maximum activity was detected. Thermostability of PhTET2 was studied as well. The enzymatic activity decay obeyed first-order kinetics and showed half-lives of 24.8 min and 10.03 h when incubated at 100 and 80 °C, respectively (Table 4).

PhTET2 Is a Metalloaminopeptidase. To further characterize the enzymatic activity, various potential inhibitors were tested. The effects of several chemical agents on PhTET2 activity are summarized in Table 5. The enzyme was clearly inhibited in the presence of EDTA, a metal ion chelating agent, and bestatin, a typical inhibitor of aminopeptidases. Weak inhibition was also detected in the presence of phosphoramidon, a metalloendopeptidases inhibitor, but only when this agent was used at a very high concentration (its effective inhibitory concentration is normally in the range 1–10 μ M). PhTET2 was insensitive to the papain and trypsin inhibitor antipain, to the chymotrypsin inhibitor chymostatin, to the cysteine protease inhibitor E-64, to the serine and cysteine protease inhibitor leupeptin, to the aspartate protease

inhibitor pepstatin, and to the serine protease inhibitors Pefabloc SC and aprotinin. Puromycin, an inhibitor of some exopeptidases, had practically no effect on the activity of PhTET2.

DISCUSSION

The PH1527 protein from *P. horikoshii* is related to the M42 peptidase family according to the classification of peptidases in evolutionary clans and families of sequence similarities proposed by Rawlings et al. (18). The members of the M42 peptidase family are widespread in all prokaryotic genomes and absent in eukaryotes. Their position in the cellular proteolysis processes remains to be clarified. Until now there are only a few of them to which a biochemical activity has been assigned, and structural studies are scarce. Family M42 includes aminopeptidases from Gram-positive bacteria such as the glutamyl aminopeptidase from *Lactococcus lactis* (GluAP) and the thermostable aminopeptidase I from *Bacillus stearothermophilus* (API). Only short N-terminal fragments are known for the two nonidentical subunits of API, but both show significant similarity to the YsdC protein from *Bacillus subtilis*. This protein is not known to be a peptidase, but it is homologous to GluAP (25) and its X-ray crystallographic structure is almost identical to that of PhTET1³ and PhTET2 (22). Broadly speaking, the outcome from the studies on M42 proteins is that they assemble in oligomeric complexes, located in the cytosol, and that their activities may differ.

We report here that the PH1527 protein forms a stable dodecameric complex in solution. The electron microscopy images revealed a shape and dimensions that are identical to the ones obtained for DAP, a member of the M42 family that was identified in *P. horikoshii* (19). We have solved the 3D structure of DAP by X-ray crystallography and electron microscopy.³ It shows that the protein assembles as a large dodecameric edifice with a tetrahedral shape. The same quaternary structure was reported in halophilic archaea for another member of the M42 family called TET (13). Therefore, in *P. horikoshii* there are two structurally related TET-like complexes. For this reason, we named DAP as PhTET1 and PH1527 as PhTET2. Almost half of the described aminopeptidases are monomers, while the remainder have oligomeric structures (34). All of the characterized M42 peptidases have multimeric structures (13, 19, 35–37). PhTET2 is a dodecamer like HmTET (13), PhTET1,³ and API (36). TET proteins are not structurally related to any other large protease in its quaternary structure, although they share a triangular shape with bovine lens leucyl aminopeptidase (bLAP), Tricorn, and Gal6 (bleomycin hydrolase) (38–40). PhTET2 seems to be self-compartmentalized, and this feature has also been recognized in some other ATP-independent exopeptidase complexes such as Gal6 and DppA (41, 42). In contrast, the molecular architectures of the *Streptomyces griseus* aminopeptidase (SGAP) and the *Aeromonas* aminopeptidase (AAP), two structurally well-characterized exopeptidases from clan MH, show that they are small monomeric metalloenzymes (43, 44).

Metallopeptidases that belong to clan MH have been described by Rawlings and Barrett (25) as containing two zinc cocatalytic metal ions. However, regarding M42 peptidases, that statement has only been experimentally con-

firmed for *P. furiosus* DAP (37). When we examined the metal dependence of PhTET2 amidolytic activity, we found that it was enhanced by Co^{2+} ion, while Zn^{2+} and Mn^{2+} ions were inhibitory and Ca^{2+} and Mg^{2+} were without effect (Table 3). Moreover, the activity of PhTET2 was strongly inhibited in the presence of the metal chelator EDTA, while the enzyme was insensitive to serine, cysteine, and aspartate protease inhibitors (Table 5). Altogether, these results indicate that PhTET2 is a metalloenzyme, but it remains unclear which metal is present in this and the other M42 peptidase catalytic sites under physiological conditions. Ando et al. (19) reported that PhTET1 was chelated with one calcium ion per monomer of protein, although removal of the calcium did not affect the enzyme activity and replacement of the calcium with zinc also showed no effect on the hydrolytic action. On the other hand, PhTET1 was strongly activated by cobalt ion, and its X-ray crystallographic structure has been modeled with two cobalt ions per catalytic site,³ although no cobalt ion was found bound to the purified protein (20). Co^{2+} activation has also been reported for GluAP (45), API (36), and *P. furiosus* DAP (37). Metalloaminopeptidases can exhibit complex metal ion dependence. For example, for AAP (belonging to family M28 in clan MH) two zinc ions are essential for full enzymatic activity; however, the addition of 1 mol of Zn^{2+} to apo-AAP provides an enzyme which is partially active, and substitution of one or both zinc ions in AAP with Co^{2+} , Cu^{2+} , or Ni^{2+} provides different magnitudes of activity that are dependent on the sequence and order of addition (46). We detected some activity when PhTET2 was assayed without Co^{2+} in the buffer (Table 3), and the same phenomenon was reported for PhTET1 (20). Furthermore, Franzetti et al. (13) performed all of their study on HmTET activity without adding any metal cation to the reaction mixtures. Therefore, a mechanism similar to that described for AAP might exist in the M42 peptidases.

PhTET2 acts optimally at pH 7.5 using Leu-pNA as a substrate, and that value agrees very well with the reported optimal pH values for GluAP (45), API (36), *P. furiosus* DAP (37), and PhTET1 (19) that are all in the range 6.5–9.0. The optimal temperature for activity of PhTET2 is around 100 °C, which is higher than the temperature optima of PhTET1 [95 °C (19)] and *P. furiosus* DAP [90 °C (37)]. The hyperthermostability of PhTET2 (Table 4) and its high activity in a broad pH range (Figure 5) make PhTET2 a clear candidate for biotechnological applications.

PhTET1 was reported to be a broad aminopeptidase with peptide deblocking activity (19). However, within peptidases of the same family, few changes in the active site environment can lead to a different type of activity. For example, family M28 in clan MH contains amino- and also carboxypeptidases. Moreover, despite high sequence identity and/or structural similarity with peptidases, some proteins display a completely different function. In this regard, and like other families in the clan, family M42 includes enzymes that are not peptidases, such as an endoglucanase from *Clostridium thermocellum* (25), and HTET was originally designated as a putative endoglucanase (17). These facts prompted us to characterize in detail the enzymatic activity of the purified PhTET2 protein complex and to compare it with the ones described for other assigned M42 peptidases. When the PhTET2 activity was assayed on small chromogenic protease

substrates and on polypeptides, we found that the protein could cleave at least 13 different amino acid residues from the N-terminus (Tables 1 and 2). Like the well-studied bLAP (47), AAP (48), and SGAP (49), PhTET2 is a fairly unspecific leucyl aminopeptidase. This feature distinguishes clearly PhTET2 from GluAP. As its name suggests, this M42 peptidase can only remove glutamyl, aspartyl, and, to a lesser extent, seryl residues from the N-terminus of peptide substrates (45). However, the broad substrate specificity of PhTET2 is similar to that of other M42 peptidases such as *P. furiosus* DAP (37), API (36), and HmTET (13). Interestingly, blocking the substrate N-terminus with an acetyl group (i.e., Ac-Leu-pNA, a typical PhTET1 substrate) prevented hydrolysis by PhTET2, indicating that PhTET2 is not a deblocking aminopeptidase, and therefore it has a different substrate specificity than the highly homologous PhTET1 (19) and *P. furiosus* DAP (37) proteins. The absence of activity against N-terminal blocked peptides has also been reported for GluAP (50) and together with the lack of measurable hydrolytic action on FITC-casein indicates that PhTET2 has a strict requirement for a free amino terminus and that it is a true exopeptidase devoid of endopeptidase activity. Moreover, PhTET2 acted on Ala-Ala-pNA, Ala-Ala-Ala-pNA, and Ala-Ala-Phe-AMC cleaving only amino acids from the N-terminus; therefore, PhTET2 seems to lack di- and tripeptidyl activity and can be classified as a strict aminopeptidase. These results are strengthened by the fact that PhTET2 activity was not affected by the presence of endoprotease inhibitors such as antipain or chymostatin, but it was inhibited by the typical aminopeptidase inhibitor bestatin (Table 5). The absence of clear puromycin inhibition can be explained by the nature of this compound: it is not a peptide, but a nucleoside, so its structure may not fit easily in the PhTET2 catalytic site. Additionally, PhTET2 seems to be unable to act on aminoacyl–proline bonds, since no cleaving of the alanyl residue was detected using Ala-Pro-pNA as a substrate. This is also a feature of GluAP (45), *P. furiosus* DAP (37), PhTET1 (19), and HmTET (13). However, although no X-Pro aminopeptidase activity is demonstrable, N-terminal prolyl residues are released by PhTET2, similar to API (36), *P. furiosus* DAP (37), and HmTET (13).

PhTET2 can act only on moderately long polypeptides such as GluAP and PhTET1 do (19, 35). HmTET was reported to cleave polypeptides up to 32 residues long (13), while *P. furiosus* DAP is already commercially used for N-terminal sequencing of acyl-blocked proteins (21, 51). The analysis of the PhTET2 action on the peptides Tub-Cter and AIT-Ad2 showed that the levels of the products do not increase in parallel and that the ratio among their areas changed with time (Figure 4; not shown). Thus, PhTET2 releases partially digested peptides that are attacked at later times. In other words, PhTET2 does not degrade peptides in a processive fashion, since the pattern of products generated varied with time. Therefore, PhTET2 initially produces a polypeptidic fragment of the peptide substrate that is degraded further at later times, as expected for nonprocessive peptidases, which detach from the polypeptide substrates after each cleavage. The results shown in Table 2 and Figure 4 also indicate that PhTET2 is not able to act as a carboxypeptidase, since no peptide fragments devoid of the first C-terminal amino acid residue(s) were detected. This finding also agrees with previous results on HmTET (13)

and PhTET1 (19).

Many metalloaminopeptidases appear to exploit their oligomeric state as part of the selection criterion for substrates, thus preventing unwanted proteolysis (52). For example, bLAP functions as hexamers. The monomers are arranged as two layers of trimers with the active sites in the interior of the oligomer (38). Without this limitation bLAP, having broad specificity, would most likely hydrolyze a large number of proteins (52). Because of this potential for unregulated proteolysis, it seems clear why the structurally related aminopeptidases AAP and SGAP function as monomers, since they are extracellular enzymes implicated in the degradation of nutritional proteins (53, 54), so their "uncontrolled" action is much more beneficial than detrimental for the cell. The sophisticated self-compartmentalized quaternary structure of PhTET1 and PhTET2 and their ability to cleave a broad set of N-terminal peptide bonds suggest that they both play a role in cytosolic protein degradation rather than in the cleaving of small dietary peptides. Having different requirements for substrate composition, they might work in a complementary way. The processing of unfolded proteins and peptides by the combined action of the 20S proteasome and the Tricorn-F1-F2-F3 complex in *Thermoplasma acidophilum* was demonstrated in vitro (7). Since no Tricorn homologue has been found in *Pyrococcus* or in *Halobacterium*, the TET system might represent a functional analogue of the Tricorn complex.

REFERENCES

- Ward, D. E., Shockley, K. R., Chang, L. S., Levy, R. D., Michel, J. K., Connors, S. B., and Kelly, R. M. (2002) Proteolysis in hyperthermophilic microorganisms, *Archaea* 1, 63–74.
- Baumeister, W., Walz, J., Zühl, F., and Seemüller, E. (1998) The proteasome: paradigm of a self-compartmentalizing protease, *Cell* 92, 367–380.
- De Mot, R., Nagy, I., Walz, J., and Baumeister, W. (1999) Proteasomes and other self-compartmentalizing proteases in prokaryotes, *Trends Microbiol.* 7, 88–92.
- Maurizi, M. R. (1987) Degradation in vitro of bacteriophage λ N protein by Lon protease from *Escherichia coli*, *J. Biol. Chem.* 262, 2696–2703.
- Kisselev, A. F., Akopian T. N., Woo, K. M., and Goldberg, A. L. (1999) The sizes of peptides generated from protein by mammalian 26 and 20S proteasomes: implications for understanding the degradative mechanism and antigen presentation, *J. Biol. Chem.* 274, 3363–3371.
- Tamura, T., Tamura, N., Cejka, Z., Hegerl, R., Lottspeich, F., and Baumeister, W. (1996) Tricorn protease: the core of a modular proteolytic system, *Science* 274, 1385–1389.
- Tamura, N., Lottspeich, F., Baumeister, W., and Tamura, T. (1998) The role of Tricorn protease and its aminopeptidase-interacting factors in cellular protein degradation, *Cell* 95, 637–648.
- Goettig, P., Groll, M., Kim, J.-S., Huber, R., and Brandstetter, H. (2002) Structures of the tricorn-interacting aminopeptidase F1 with different ligands explain its catalytic mechanism, *EMBO J.* 21, 5343–5352.
- Fukasawa, K., Fukasawa, K. M., Kanai, M., Fujii, S., Hirose, J., and Harada, M. (1998) Dipeptidyl peptidase III is a zinc metallo-exopeptidase: molecular cloning and expression, *Biochem. J.* 329, 275–282.
- Tomkinson, B. (1999) Tripeptidyl peptidases: enzymes that count, *Trends Biochem. Sci.* 24, 355–359.
- Geier, E., Pfeifer, G., Wilm, M., Lucchiari-Hartz, M., Baumeister, W., Eichmann, K., and Niedermann, G. (1999) A giant protease with potential to substitute for some functions of the proteasome, *Science* 283, 978–981.
- Wang, E. W., Kessler, B. K., Borodovsky A., Cravatt, B. F., Bogoy, M., Ploegh, H. L., and Glas, R. (2000) Integration of the ubiquitin-proteasome pathway with a cytosolic oligopeptidase activity, *Proc. Natl. Acad. Sci. U.S.A.* 97, 9990–9995.
- Franzetti, B., Schoehn, G., Hernandez, J.-F., Jaquinod, M., Ruigrok, R. W. H., and Zaccari, G. (2002) Tetrahedral aminopeptidase: a novel large protease complex from Archaea, *EMBO J.* 21, 2132–2138.
- Constam, D. B., Tobler, A. R., Rensing-Ehl, A., Kemler, I., Hersh, L. B., and Fontana, A. (1995) Puromycin-sensitive aminopeptidase: sequence analysis, expression, and functional characterization, *J. Biol. Chem.* 270, 26931–26939.
- Beninga, J., Rock, K. L., and Goldberg, A. L. (1998) Interferon- γ can stimulate post-proteasomal trimming of the N terminus of an antigenic peptide by inducing leucine aminopeptidase, *J. Biol. Chem.* 273, 18734–18742.
- Saric, T., Beninga, J., Graef, C. I., Akopian, T. N., Rock, K. L., and Goldberg, A. L. (2001) Major histocompatibility complex class I-presented antigenic peptides are degraded in cytosolic extracts primarily by thimet oligopeptidase, *J. Biol. Chem.* 276, 36474–36481.
- Ng, W. V., et al. (2000) Genome sequence of *Halobacterium* species NRC-1, *Proc. Natl. Acad. Sci. U.S.A.* 97, 12176–12181.
- Rawlings, N. D., Tolle, D. P., and Barrett, A. J. (2004) MEROPS: the peptidase database, *Nucleic Acids Res.* 32, D160–D164.
- Ando, S., Ishikawa, K., Ishida, H., Kawarabayashi, Y., Kikuchi, H., and Kosugi, Y. (1999) Thermostable aminopeptidase from *Pyrococcus horikoshii*, *FEBS Lett.* 447, 25–28.
- Onoe, S., Ando, S., Ataka, M., and Ishikawa, K. (2002) Active site of deblocking aminopeptidase from *Pyrococcus horikoshii*, *Biochem. Biophys. Res. Commun.* 290, 994–997.
- Tsunasawa, S. (1998) Purification and application of a novel N-terminal deblocking aminopeptidase (DAP) from *Pyrococcus furiosus*, *J. Protein Chem.* 17, 521–522.
- Russo, S., and Baumann, U. (2004) Crystal structure of a dodecameric tetrahedral-shaped aminopeptidase, *J. Biol. Chem.* 279, 51275–51281.
- Schuck, P., Perugini, M. A., Gonzales, N. R., Howlett, G. J., and Schubert, D. (2002) Size-distribution analysis of proteins by analytical ultracentrifugation: strategies and application to model systems, *Biophys. J.* 82, 1096–1111.
- Aristoy, M. C., and Toldrá, F. (1991) Deproteinization techniques for HPLC amino acid analysis in fresh pork muscle and dry-cured ham, *J. Agric. Food Chem.* 39, 1792–1795.
- Rawlings, N. D., and Barrett, A. J. (2004) Introduction: metallo-peptidases and their clans, in *Handbook of Proteolytic Enzymes* (Barrett, A. J., Rawlings, N. D., and Woessner, J. F., Eds.) 2nd ed., pp 231–268, Elsevier, London.
- Vallee, B. L., and Auld, D. S. (1993) New perspective on zinc biochemistry: cocatalytic sites in multi-zinc enzymes, *Biochemistry* 32, 6493–6500.
- Singh, H., and Kalnitsky, G. (1980) α -N-Benzoylarginine- β -naphthylamide hydrolase, an aminoendopeptidase from rabbit lung, *J. Biol. Chem.* 255, 369–374.
- Taylor, A. (1993) Aminopeptidases: structure and function, *FASEB J.* 7, 290–298.
- Koldamova, R. P., Lefterov, I. M., Gadjeva, V. G., and Lazo, J. S. (1998) Essential binding and functional domains of human bleomycin hydrolase, *Biochemistry* 37, 2282–2290.
- Turk, V., Turk, B., and Turk, D. (2001) Lysosomal cysteine proteases: facts and opportunities, *EMBO J.* 20, 4629–4633.
- Chandu, D., Kumar, A., and Nandi, D. (2003) PepN, the major Suc-LLVY-AMC-hydrolysing enzyme in *Escherichia coli*, displays functional similarity with downstream processing enzymes in Archaea and Eukarya, *J. Biol. Chem.* 278, 5548–5556.
- Akopian, T. N., Kisselev, A. F., and Goldberg, A. L. (1997) Processive degradation of proteins and other catalytic properties of the proteasome from *Thermoplasma acidophilum*, *J. Biol. Chem.* 272, 1791–1798.
- Thompson, M. W., Singh, S. K., and Maurizi, M. R. (1994) Processive degradation of proteins by the ATP-dependent Clp protease from *Escherichia coli*: requirement for the multiple array of active sites in ClpP but not ATP hydrolysis, *J. Biol. Chem.* 269, 18209–18215.
- Schürer, G., Lanig, H., and Clark, T. (2004) *Aeromonas proteolytica* aminopeptidase: an investigation of the mode of action using a quantum mechanical/molecular mechanical approach, *Biochemistry* 43, 5414–5427.
- Bacon, C. L., Jennings, P. V., Fhaolain, I. N., and O’Cuinn, G. (1994) Purification and characterization of an aminopeptidase A from cytoplasm of *Lactococcus lactis* subsp. *cremoris* AM2, *Int. Dairy J.* 4, 503–519.

36. Motoshima, H., and Kaminogawa, S. (2004) *Bacillus* aminopeptidase I, in *Handbook of Proteolytic Enzymes* (Barrett, A. J., Rawlings, N. D., and Woessner, J. F., Eds.) 2nd ed., pp 968–970, Elsevier, London.
37. Tsunasawa, S. (2004) N-terminal deblocking aminopeptidase (*Pyrococcus furiosus*), in *Handbook of Proteolytic Enzymes* (Barrett, A. J., Rawlings, N. D., and Woessner, J. F., Eds.) 2nd ed., pp 970–972, Elsevier, London.
38. Burley, S. K., David, P. R., Taylor, A., and Lipscomb, W. N. (1990) Molecular structure of leucine aminopeptidase at 2.7-Å resolution, *Proc. Natl. Acad. Sci. U.S.A.* 87, 6878–6882.
39. Joshua-Tor, L., Xu, H. E., Johnston, S. A., and Rees, D. C. (1995) Crystal structure of a conserved protease that binds DNA: the bleomycin hydrolase, Gal6, *Science* 269, 945–950.
40. Brandstetter, H., Kim, J.-S., Groll, M., and Huber, R. (2001) Crystal structure of the tricorn protease reveals a protein disassembly line, *Nature* 414, 466–470.
41. Lupas, A., Flanagan, J. M., Tamura, T., and Baumeister, W. (1997) Self-compartmentalizing proteases, *Trends Biochem. Sci.* 22, 399–404.
42. Remaut, H., Bompard-Gilles, C., Goffin, C., Frère, J.-M., and van Beeumen, J. (2001) Structure of the *Bacillus subtilis* D-aminopeptidase DppA reveals a novel self-compartmentalizing protease, *Nat. Struct. Biol.* 8, 674–678.
43. Greenblatt, H. M., Almog, O., Maras, B., Spungin-Bialik, A., Barra, D., Blumberg, S., and Shoham, G. (1997) *Streptomyces griseus* aminopeptidase: X-ray crystallographic structure at 1.75 Å resolution, *J. Mol. Biol.* 265, 620–636.
44. Chevrier, B., Schalk, C., D'Orchymont, H., Rondeau, J. M., Moras, D., and Tarnus, C. (1994) Crystal structure of *Aeromonas proteolytica* aminopeptidase: a prototypical member of the co-catalytic zinc enzyme family, *Structure* 2, 283–291.
45. Niven, G. W. (2004) Glutamyl aminopeptidase (*Lactococcus*), in *Handbook of Proteolytic Enzymes* (Barrett, A. J., Rawlings, N. D., and Woessner, J. F., Eds.) 2nd ed., pp 965–968, Elsevier, London.
46. Chen, G. J., Edwards, T., D'souza, V. M., and Holz, R. C. (1997) Mechanistic studies on the aminopeptidase from *Aeromonas proteolytica*: a two-metal ion mechanism for peptide hydrolysis, *Biochemistry* 36, 4278–4286.
47. Spector, A. (1963) Lens aminopeptidase. I: purification and properties, *J. Biol. Chem.* 238, 1353–1357.
48. Wagner, F. W., Wilkes, S. H., and Prescott, J. M. (1972) Specificity of *Aeromonas* aminopeptidase toward amino acid amides and dipeptides, *J. Biol. Chem.* 247, 1208–1210.
49. Ben-Meir, D., Spungin, A., Ashkenazi, R., and Blumberg, S. (1993) Specificity of *Streptomyces griseus* aminopeptidase and modulation of activity by divalent metal ion binding and substitution, *Eur. J. Biochem.* 212, 107–112.
50. Exterkate, F. A., and de Veer, G. J. C. M. (1987) Purification and some properties of a membrane-bound aminopeptidase A from *Streptococcus cremoris*, *Appl. Environ. Microbiol.* 53, 577–583.
51. Kamp, R. M., Tsunasawa, S., and Hirano, H. (1998) Application of new deblocking aminopeptidase from *Pyrococcus furiosus* for microsequence analysis of blocked proteins, *J. Protein Chem.* 17, 512–513.
52. Lowther, W. T., and Matthews, B. W. (2002) Metalloaminopeptidases: common functional themes in disparate structural surroundings, *Chem. Rev.* 102, 4581–4607.
53. Prescott, J. M., and Wilkes, S. H. (1976) *Aeromonas* aminopeptidase, *Methods Enzymol.* 45, 530–543.
54. Vosbeck, K. D., Chow, K. F., and Awad, W. M. J. (1973) The proteolytic enzymes of the K-1 strain of *Streptomyces griseus* obtained from a commercial preparation (Pronase): purification and characterization of the aminopeptidases, *J. Biol. Chem.* 248, 6029–6034.

BI047736J